

calsequestrin 1 (Casq1) and its fusion constructs to terminal cisternae of the SR, we devised an alternative approach: the fusion of murine Casq1 and D4cpv - a cameleon of high dynamic range and affinity adequate for the SR (Palmer, Chem & Bio 2006) - was expressed in the FDB of live adult mice. The fusion protein expressed well, localizing largely to terminal cisternae. Calibrations *in situ* revealed a good dynamic range of its Ca^{2+} -dependent ratio signal ($R_{\text{max}}/R_{\text{min}} = 4$). Sensor affinity is being measured using untargeted sensor, expressed in the cytosol, or purified sensor in solution. Assuming a $K_d = 240 \mu\text{M}$, the resting $[\text{Ca}^{2+}]_{\text{SR}}$ was 0.6-1 mM in 20 cells. Consistent with the kinetics of the related sensor D1 in solution ($k_{\text{on}} = 256 \text{ s}^{-1}$, Palmer, PNAS 2004), D4cpv signals rapidly followed the decrease in $[\text{Ca}^{2+}]_{\text{SR}}$ that results from Ca^{2+} release upon voltage-clamp depolarization. Potential interference by the presence of Casq in the fused sensor was minimized by using a deletion mutant of Casq1 as targeting sequence. A first conclusion is that long-lasting depolarization may reduce $[\text{Ca}^{2+}]_{\text{SR}}$ below 10% of resting value. From the Casq1-D4cpv-monitored $[\text{Ca}^{2+}]_{\text{SR}}$ we derived the SR Ca buffering power -ratio of total/free $[\text{Ca}^{2+}]_{\text{SR}}$ - and found that it decreases upon depletion of SR Ca. As shown elsewhere (Sztrytey et al, this meeting), this anomalous buffering feature depends on the presence of calsequestrin inside the SR. Funded by NIAMS/NIH and MDA.

1539-Pos

Ca Depletion and Ablation of Calsequestrin Similarly Increase the Evacuability of the Ca Store of Skeletal Muscle

Monika Sztrytey¹, Leandro Royer², Carlo Manno¹, Jingsong Zhou¹, Björn Knollmann³, Paul D. Allen⁴, Feliciano Protasi⁵, **Eduardo Rios¹**.

¹Rush University, Chicago, IL, USA, ²Université Bordeaux 2, Bordeaux, France, ³Vanderbilt University, Nashville, TN, USA, ⁴Brigham and Women's Hospital, Boston, MA, USA, ⁵CeSI-Univ. G. d'Annunzio, Chieti, Italy.

At ~200 ms during a voltage pulse the flux of Ca release induced by membrane depolarization of mouse muscle exhibits a characteristic acceleration of decay, or shoulder, associated with SR depletion. The shoulder reflects an increase in evacuability E , an index calculated from the flux, equal to the ratio of release permeability, P , and SR Ca buffering power, B (Royer, J Physiol 2008). To tell whether this rise in E reflects an increase in P or a decrease in B we recorded flux and calculated E in FDB cells from mice lacking either calsequestrin 1 (Paolini, J Physiol 2007) or both isoforms of calsequestrin, the main Ca buffer in the SR. In both null mice the flux waveform lacked the shoulder, and E was elevated, adopting from the start the high value reached upon depletion in the wild-type. Hence, low E requires the presence of calsequestrin inside the store. In aqueous solutions the Ca-binding capacity of calsequestrin decreases at low $[\text{Ca}^{2+}]$ (Park, JBC 2005). Therefore we hypothesized that the increase in E during a pulse is due to an analogous effect of decaying $[\text{Ca}^{2+}]_{\text{SR}}$ on the Ca-buffering capacity of calsequestrin *in situ*. Confirming the hypothesis, when the SR was depleted in cells voltage-clamped in zero Ca external solutions, the kinetics of release became similar to that of calsequestrin-null cells, featuring no shoulder and a high initial E .

Low evacuability simply implies that the SR may release Ca with minimal decrease in $[\text{Ca}^{2+}]_{\text{SR}}$, therefore conserving the driving force for subsequent release. A functional correlate is the ability to sustain Ca release and Ca transients during the high frequency activation of physiological contractions and exercise. Funded by NIAMS/NIH and MDA.

1540-Pos

Compromised Ca^{2+} Sparks Signaling in the Skeletal Muscle of Diabetic Type 2 Mice

Andoria Tjondrokoemo, Noah Weisleder, Jianjie Ma. UMDNJ, Piscataway, NJ, USA.

Type 2 diabetes mellitus (DM) is a prevailing epidemic metabolic disease that is mainly characterized as insulin resistant and β -cell dysfunction that leads to aberrant glucose metabolism in skeletal muscle. Altered homeostatic capacity for effective $[(\text{Ca}^{2+})_i]$ signaling may underlie the reduced contractile dysfunction associated with DM. Measurement of osmotic stress induced Ca^{2+} sparks on the young control wild-type (WT) C57Bl/6J and db/db type 2 DM mice models show that Ca^{2+} sparks frequency is significantly attenuated in the db/db fibers (36 ± 6 events/min) when compared to control (107 ± 7 events/min). These findings suggest that Ca^{2+} sparks can be used as a readout of the Ca^{2+} handling characteristic of skeletal muscle fibers, as we have previously shown in muscular dystrophy and aging muscle. This idea is supported with additional studies that show therapeutic agents for diabetes can modulate Ca^{2+} spark signaling. Treatment of 10 nM glucagon like peptide 1 (GLP1), an incretin hormone associated with increased insulin secretion, significantly increases the

Ca^{2+} sparks frequency in the db/db muscle (120 ± 10 events/min), similar to the level of untreated WT. The plot of Ca^{2+} sparks localization shows that treatment of GLP1 in either db/db or WT does not alter the peripheral subsarcolemmal distribution of Ca^{2+} sparks, implying that the factor responsible for maintaining Ca^{2+} sparks localization near the membrane remains intact. Studies in β -cell suggests that increased specific intracellular signaling cascade can be regulated by GLP-1. We find that these signaling cascades can also contribute to the activation of Ca^{2+} sparks in skeletal muscle.

Local Calcium Signaling

1541-Pos

A Technique to Accelerate Stochastic Markov Chain Monte Carlo Simulations of Calcium-Induced Calcium Release in Cardiac Myocytes

George Williams¹, Aristide Chikando², Gregory Smith³, Mohsin Saleet Jafri¹.

¹George Mason University, Fairfax, VA, USA, ²University of Maryland Biotechnology Institute, Baltimore, MD, USA, ³College of William and Mary, Williamsburg, VA, USA.

Considerable insight into intracellular calcium (Ca) responses has been obtained through the development of whole cell models that are based on molecular mechanisms, e.g., the kinetics of intracellular Ca channels and the feedback of Ca upon these channels. However, a limitation of most deterministic whole cell models to date is the assumption that channels are globally coupled by a "common pool" of [Ca], when in fact channels experience localized "domains" [Ca]. More realistic stochastic Monte Carlo simulations are capable of capturing the influence of local [Ca] on channel gating. Unfortunately, such local control models of calcium-induced calcium release (CICR) are computationally expensive due to the explicit representation of 10,000 to 20,000 release sites, each containing 50 to 300 stochastically gating Ca channels. Here, we present a novel technique called vectorized gating that optimizes the solution time of Markov chain Monte Carlo (MCMC) simulations. Additionally, as this technique leverages vector and matrix algebra it can benefit from the use of the advanced NVIDIA TESLA graphics processing unit (GPU) to further accelerate MCMC models. NVIDIA TESLA cards utilize the parallel nature of the NVIDIA CUDA architecture and are powered by up to 960 parallel processing cores. Benchmark simulations indicate that the GPU-enhanced vectorized gating technique is significantly faster than CPU-only driven calculations. The vectorized gating technique also lends itself to the direct calculation of an adaptive time step which optimizes speed while maintaining numerical stability. These computational enhancements are utilized to facilitate study of sarcoplasmic reticulum (SR) leak from clusters of ryanodine receptor (RyR) Ca channels in cardiac myocytes.

1542-Pos

In Situ Calibration of Cytoplasmic and Nucleoplasmic Calcium Concentration in Adult Rat and Mouse Cardiac Myocytes

Senka V. Ljubojevic, Stefanie Walther, Burkert M. Pieske, Jens Kockskämper.

Medical University of Graz, Graz, Austria.

Quantifying subcellularly resolved Ca^{2+} signals in cardiac myocytes is essential for understanding Ca^{2+} fluxes in excitation-contraction and excitation-transcription coupling. Translation of changes in Ca^{2+} -dependent fluorescence into changes in $[\text{Ca}^{2+}]$ relies on the indicator's behavior *in situ*, but properties of fluorescent indicators in different intracellular compartments may differ. Thus, we determined the *in situ* calibration of a frequently used Ca^{2+} indicator, Fluo-4, and evaluated its use in reporting cytoplasmic and nucleoplasmic Ca^{2+} signals in isolated cardiac myocytes.

Calibration solutions were made by mixing known quantities of EGTA and CaEGTA solutions and the free $[\text{Ca}^{2+}]$ was confirmed with a Ca^{2+} -sensitive electrode. Solutions contained metabolic inhibitors and cyclopiazonic acid (5 μM) to block active Ca^{2+} transport and the Ca^{2+} ionophore A-23187 (10 μM) to allow equilibration of $[\text{Ca}^{2+}]$ between bath solution and cell interior. Ventricular rat and mouse myocytes were loaded with Fluo-4/AM (8 μM , 20 min). Fluo-4 fluorescence (excitation/emission: 488/>505 nm) was recorded using a Nipkow dual disc-based confocal microscope.

Concentration-response curves were obtained and a significant difference in the apparent Ca^{2+} binding affinities (K_d) of Fluo-4 between cytoplasmic ($993 \pm 56 \text{ nM}$; $1026 \pm 65 \text{ nM}$) and nucleoplasmic ($1211 \pm 73 \text{ nM}$; $1251 \pm 71 \text{ nM}$) compartments was observed for both mouse and rat cells, respectively (both $n=15$, $P<0.01$). The established curves were used to transform raw Fluo-4 fluorescence signals during electrically stimulated $[\text{Ca}^{2+}]$ transients

(1 Hz, room temperature) into nucleoplasmic and cytoplasmic $[Ca^{2+}]$. There was a significant difference in diastolic (121 ± 24 nM vs 149 ± 35 nM; 99 ± 17 nM vs 121 ± 26 nM) and systolic (420 ± 148 nM vs 364 ± 102 nM; 787 ± 172 nM vs 491 ± 157 nM) $[Ca^{2+}]$ between cytoplasmic and nucleoplasmic compartments in mouse and rat cells, respectively (both $n=15$; $P<0.01$). The results reveal that, in cardiac myocytes, the Ca^{2+} -dependent fluorescent properties of Fluo-4 differ between cytoplasm and nucleoplasm and that significant differences between cytoplasmic and nucleoplasmic $[Ca^{2+}]$ exist during diastole as well as systole.

1543-Pos

Control of Ca Release Synchrony by Action Potential Configuration in Murine Cardiomyocytes

Johan Hake¹, Guro F. Jølle^{2,3}, Halvor K. Mørk^{2,3}, Ivar Sjaastad^{2,3}, Ole M. Sejersted^{2,3}, William E. Louch^{2,3}, Glenn T. Lines¹.

¹Simula Research Laboratory, Lysaker, Norway, ²Institute for Experimental Medical Research, Oslo University Hospital - Ullevål, Oslo, Norway.

³Centre for Heart Failure Research, Faculty of Medicine, University of Oslo, Oslo, Norway.

Spatially non-uniform or "dyssynchronous" sarcoplasmic reticulum (SR) Ca release has been reported in cardiomyocytes from failing hearts. Using a murine model of congestive heart failure (CHF) following myocardial infarction, we investigated whether altered action potential (AP) configuration promotes release dyssynchrony. We observed that APs (1 Hz) were prolonged in cardiomyocytes isolated from the viable septum of CHF hearts, compared to and sham-operated controls (SHAM). Representative AP recordings were included in a detailed computational model of the Ca dynamics in the dyad. The model predicted reduced driving force for L-type Ca current and more dyssynchronous opening of ryanodine receptors during stimulation with the CHF AP than the SHAM AP. These predictions were confirmed in isolated cardiomyocyte experiments, when cells were alternately stimulated by SHAM and CHF AP voltage-clamp waveforms. However, when a train of like APs was used as the voltage stimulus, the SHAM and CHF AP produced a similar Ca release pattern. In this steady-state condition, both modeling and cell experiments showed that greater integrated Ca entry during the CHF AP lead to increased SR Ca content. We modeled the effect of increased SR Ca content by increasing the Ca sensitivity of the ryanodine receptor, which we observed increased the synchrony of ryanodine receptor activation. Thus, at steady-state, Ca release synchrony was maintained during the CHF AP as greater ryanodine sensitivity offset the de-synchronizing effects of reduced driving force for Ca entry. Our results suggest that dyssynchronous Ca release in failing mouse myocytes results from alterations such as T-tubule re-organization, and not electrical re-modeling.

1544-Pos

Imaging of the Ryanodine Receptor Distribution in Rat Cardiac Myocytes with Optical Single Channel Resolution

David Baddeley¹, Isuru D. Jayasinghe¹, Leo Lam¹, Sabrina Rossberger^{1,2}, Mark B. Cannell¹, Christian Soeller¹.

¹University of Auckland, Auckland, New Zealand, ²University of Heidelberg, Heidelberg, Germany.

We have applied a new optical super-resolution technique based on single molecule localisation to examine the peripheral distribution of a cardiac signalling protein, the ryanodine receptor (RyR), in rat ventricular myocytes. Using high-resolution antibody labeling data we show that the new imaging approach, termed localization microscopy, can give novel insight into the distribution of large proteins, with optical single channel resolution. We present, to our knowledge, the first direct data showing evidence for a two-dimensional array-like arrangement of RyRs in cardiac muscle. Morphological analysis of peripheral RyR clusters in the surface membrane revealed a mean size of ~14 RyRs per cluster, almost an order of magnitude smaller than previously estimated. Clusters were typically not circular (as previously assumed) but elongated with an average aspect ratio of 1.9. Edge-to-edge distances between adjacent RyR clusters were often less than 50 nm suggesting that peripheral RyR clusters may exhibit strong inter-cluster signalling. The cluster size varied widely and followed a near-exponential distribution. We show that this distribution is compatible with a stochastic cluster assembly process and construct simple cluster growth models that generate size distributions very similar to our experimental observations. Based on the placement and morphology of RyR clusters we suggest that calcium sparks may be the result of the concerted activation of several clusters forming a functional 'supercluster' whose gating is controlled by both cytosolic and sarcoplasmic reticulum luminal calcium levels. The new imaging approach can be extended to other cardiac proteins and should yield novel insight into excitation-contraction coupling and the control of cardiac contractility.

1545-Pos

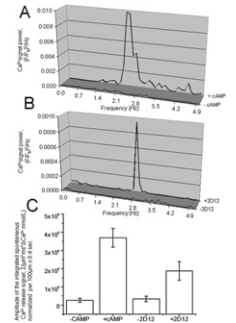
Synchronization of Spontaneous Stochastic RyR Activation in Ventricular Myocytes (VM) by Camp or Disengagement of Phospholambam (PLB) From SERCA2

Syevda Sirenko^{1,2}, Tatiana M. Vinogradova¹, Larry R. Jones³, Victor Maltsev¹, Edward G. Lakatta¹.

¹Laboratory of Cardiovascular Science, National Institute on Aging, NIH, Baltimore, MD, USA, ²MedStar Research Institute, Baltimore, MD, USA,

³Krannert Institute of Cardiology, Indianapolis, Indianapolis, IN, USA.

Stochastic RyR activation underlies Ca^{2+} sparks in VM. Here we show that in saponin "skinned" VM, bathed in 100 nM Ca^{2+} at 35°C, cAMP converts this stochastic spontaneous RyR activation (Ca^{2+} sparks-confocal linescan imaging) into synchronized, rhythmic RyR activation (Fig. A) about an average dominant frequency 2.2 ± 0.13 Hz ($n=3$). Of note, cAMP does not alter the SR Ca^{2+} load assessed by the rapid application of caffeine (107 ± 17.3 nM Ca^{2+} $n=9$ prior and 121 ± 19.3 nM Ca^{2+} $n=3$ during cAMP exposure). When Ca^{2+} pumping into SR is selectively accelerated by a PLB antibody (2D12, 0.013 mg/ml) that disengages PLB from SERCA2, stochastic RyR Ca^{2+} release becomes rhythmic (Fig. B) about an average dominant frequency of 2.6 ± 0.21 Hz ($n=5$). The amplitude of the integrated spontaneous Ca^{2+} release signal during any given epoch increases when stochastic RyR activation becomes synchronized, i.e. converted to rhythmic activation (Fig. C). This cAMP-generated rhythmicity of spontaneous RyR activation of VM mimics rhythmic spontaneous diastolic Ca^{2+} releases in sinoatrial nodal pacemaker cells which have a basal high level of intrinsic cAMP-dependent signaling.



1546-Pos

Subcellular Mechanisms of Early Impaired Calcium Homeostasis with Chronic Beta₁-Adrenergic Stimulation in Mice

Frank R. Heinzel¹, Shelina Khan², Patrick Freidl¹, Simon Sedej¹,

Felix Hohendanner¹, Paulina Wakula¹, Brigitte Korff², Stefan Engelhardt³, Burkert Pieske¹.

¹Medical University of Graz, Graz, Austria, ²University of Göttingen, Göttingen, Germany, ³Institute of Pharmacology and Toxicology, TU Munich, Munich, Germany.

Chronic beta-adrenergic stimulation leads to heart failure (HF). In mice over-expressing beta1-adrenoceptors (TG), increased diastolic Ca load in cardiomyocytes at early age is pivotal for the development of HF. The mechanisms underlying intracellular Ca dysregulation are unclear. We examined cytosolic Ca transients (Fluo4-AM, field stimulation), Na-Ca-exchanger (NCX) function and protein expression, cytosolic Na (SBFI) and T-tubular structures (Di8-ANEPPS) in cardiomyocytes from young (8-16 wks) TG mice and wildtype (WT) littermates.

Results: Systolic $[Ca]$ amplitude was unchanged, time to peak $[Ca]$ (140 ± 5 vs. 127 ± 3 ms) and $[Ca]$ decay (time constant, tau, 223 ± 16 vs. 182 ± 9 ms) were significantly prolonged in TG vs. WT. Diastolic Ca leak from the SR (quantified as tetracaine-sensitive change in diastolic $[Ca]$ or diastolic Ca spark frequency) was unchanged. However, cytosolic Ca removal by NCX during caffeine application was significantly slower (tau, 3683 ± 337 in TG vs. 2304 ± 272 ms in WT), indicating reduced forward mode NCX activity. NCX protein expression was unchanged. Preliminary results indicate increased cytosolic $[Na]$ in young TG. Furthermore, confocal line scans revealed delayed (> 15 ms until half-maximal) systolic Ca release in 24.7 ± 2.6 (TG) vs. 4.6 ± 1.4 (WT) of the intracellular regions ($n=32$ and 31 cells, resp., $p<0.01$). The extent of dyssynchronous Ca release correlated with time to peak systolic $[Ca]$ ($R=0.51$, $P<0.001$) and was associated with a lower density and increased irregularity of T-tubules in TG ($22.8 \pm 1.6\%$ of cell volume in TG vs. $26.1 \pm 2.5\%$ in WT). **In summary,** in early HF remodeling with chronic beta1-adrenergic stimulation, slowed cytosolic Ca clearance is not related to increased diastolic SR Ca leak but associated with decreased NCX forward mode activity, which may be related to increased cytosolic $[Na]$. Reduced T-tubule density with dyssynchronous, slowed systolic Ca release additionally contribute to increased cytosolic Ca load.

1547-Pos

Rational Design and Structural Analysis of Ca^{2+} Biosensor and Application in Skeletal Muscle Cells

Shen Tang, Hing-Cheung Wong, Jin Zou, Yun Huang, Jenny J. Yang. Georgia State University, Atlanta, GA, USA.

Quantitative and real-time detection of Ca^{2+} signaling in internal Ca^{2+} store sarcoplasmic reticulum (SR) of skeletal muscle cells is essential to explore